BIOLOGY OF REPRODUCTION 46, 817–828 (1992)

Distribution of the Microtubule-Dependent Motors Cytoplasmic Dynein and Kinesin in Rat Testis[1]

ERIC S. HALL, JULIA EVELETH, CHENGYU JIANG, DARLENE M. REDENBACH, and KIM BOEKELHEIDE[2]

Department of Pathology and Laboratory Medicine, Brown University, Providence, Rhode Island 02912

ABSTRACT

To examine the possible role of microtubule-based transport in testicular function, we used immunofluorescent techniques to study the presence and localization of the microtubule mechanoenzymes cytoplasmic dynein (a slow-growing end-directed motor) and kinesin (a fast-growing end-directed motor) within rat testis. Cytoplasmic dynein immunofluorescence was observed in Sertoli cells during all stages of spermatogenesis, with a peak in apical cytoplasm during stages IX-XIV. Cytoplasmic dynein immunofluorescence was also localized within Sertoli cells to steps 9–14 (stages IX-XIV) germ cell-associated ectoplasmic specializations. In germ cells, cytoplasmic dynein immunofluorescence was observed in manchettes of steps 15–17 (stages I-IV) spermatids, and small, hollow circular structures were seen in the cytoplasm of step 17 and step 18 spermatids during stages V and VI. Kinesin immunofluorescence was observed in manchettes of steps 10–18 spermatids (stages X-VI). The stage-dependent apical Sertoli cell cytoplasmic dynein immunofluorescence, in conjunction with the previously reported orientation of Sertoli cell microtubules (slow-growing ends toward the lumen) and peak secretion of androgen-binding protein and transferrin, is consistent with the hypothesis that cytoplasmic dynein is involved in Sertoli cell protein transport and secretion. Further, the localization of cytoplasmic dynein and kinesin to manchettes is consistent with current hypotheses concerning manchette function.

INTRODUCTION

Mammalian Sertoli cells provide the nutritional, hormonal, and structural environment necessary for spermatogenesis. Specialized tight junctions between adjacent Sertoli cells form the blood-testis barrier, which isolates germ cells in the adluminal compartment from the interstitial fluid [1, 2]. Sertoli cells provide nutrients and hormones by secreting seminiferous tubule fluid (STF) [3]. STF contains a number of Sertoli cell-secreted proteins including androgen-binding protein [4, 5], transferrin [6], ceruloplasmin [7], acidic glycoprotein [7], and inhibin [8, 9]. The secretion of many of these proteins varies during different stages of spermatogenesis. The rat seminiferous epithelium has fourteen morphologically distinct stages culminating in the release of mature sperm at the end of stage VIII [10]. Sertoli cell secretion of androgen-binding protein peaks during stages IX-XII [11], and transferrin is secreted at highest levels during stages VIII-XII [11].

Protein transport and secretion is a complex process involving endoplasmic reticulum, Golgi apparatus, transport and secretory vesicles, cell membrane components, and the cytoskeleton. Microtubules are involved in protein secretion by a number of cell types [12–14], and may act as tracks for vesicle and organelle transport [15–18]. Microtubules are composed of tubulin subunits, which preferentially polymerize to one end of microtubules, giving them fast-growing [+] and slow-growing [−] ends [19]. The majority (greater than 93%) of microtubules in Sertoli cells are oriented with their [+] ends towards the cell nucleus and their [−] ends towards the lumen of the seminiferous tubule [20]. Thus, the bulk transport of STF constituents must be towards the [−] ends of the microtubules. In contrast to Sertoli cells, axons have microtubules oriented with [−] ends towards the nucleus [21, 22]. Microtubule-dependent transport in Sertoli cells probably involves molecules that can bind to and move along microtubules. Cytoplasmic dynein and kinesin are two families of microtubule-based motors that bind tightly to microtubules in the absence of ATP and possess ATPase activity. In addition, when these proteins are adsorbed to glass coverslips in the presence of ATP, they can transport microtubules along the surface of the coverslip [23–25].

Kinesin was first isolated from squid axoplasm [24, 25] and has since been isolated from *Drosophila* [26], sea urchin eggs [27], bovine adrenal tissue [28], chick fibroblasts [29], HeLa cells [30], and rat liver [31]. It is composed of two heavy and two light chains of 124 and 64 kDa, respectively, with a total length of around 80 nm [24, 25, 27]. Kinesin is a unidirectional motor moving towards the [+] end of microtubules [32]. Kinesin may be involved in fast axonal transport in axons [33, 34], mitotic spindle movement in sea urchins [27, 35], and the formation of tubulovesicular networks [29, 36].

Cytoplasmic dynein was first isolated from sea urchins [37] and has since been isolated from *Caenorhabditis elegans* [38]; *Reticulomyxa* [39]; *Dictyostelium* [40]; *Paramecium* [41]; squid axons [42]; HeLa cells [43]; and rat liver, testes, and brain [31, 44, 45]. Cytoplasmic dynein moves unidirectionally towards the [−] end of microtubules [23] and has been implicated in organelle transport [39, 46–48] and mitotic spindle rearrangements [49, 50]. Additionally,

Accepted December 19, 1991.
Received October 2, 1991.
[1]Supported by PHS R01 ES05033 and K04 ES00193.
[2]Correspondence: Kim Boekelheide, M.D., Ph.D., Department of Pathology and Laboratory Medicine, Box G-B518, Providence, RI 02912. FAX: (401) 863-1971.

the translocation of maturing spermatids to the seminiferous tubule lumen from a basal location during stages V-VI [10] has been hypothesized to involve cytoplasmic dynein and its interactions with ectoplasmic specializations and microtubules [20, 51–54].

Ectoplasmic specializations consist of a sandwich of actin filaments between Sertoli cell membrane and smooth endoplasmic reticulum adjacent to sites of intercellular adhesion [1, 51, 55–57]. They form basally, in regions of intercellular contact between neighboring Sertoli cells, where they contribute to the blood-testis barrier. Ectoplasmic specializations also form in Sertoli cells adjacent to spermatids during elongation and disappear just prior to spermiation [58, 59]. The observed association of ectoplasmic specializations with intercellular adhesion junctions, along with other biochemical and morphological evidence, suggests that they are involved in intercellular adhesion [51]. In addition, because of the observed cross-links between ectoplasmic specializations and neighboring microtubules and their association with intermediate filaments, ectoplasmic specializations have been proposed to be involved in positioning spermatids within the seminiferous epithelium [20, 51–54].

Another prominent microtubule structure in the testis is the manchette, which consists of parallel, cross-linked arrays of microtubules extending from the nuclear ring of the maturing elongate spermatid towards the lumen of the seminiferous epithelium. Manchettes first form within the spermatid cytoplasm as they begin to elongate and begin to break up as spermatids are translocated through the seminiferous epithelium during stages IV-VI [60]. During disassembly, fragments of manchettes have been observed in the cytoplasm of horse and cat spermatids [61, 62]. Ultrastructural observations from mutant mice and chemically disrupted manchette models indicate that manchettes may be involved in spermatid nuclear reshaping [63–65], although chromatin condensation may also be important in this process [66, 67]. The observed association of cytoplasmic vesicles with manchette microtubules [66, 68] has led to an additional hypothesis that manchettes "may serve as a track or conveyor along which the cytoplasm is translocated from the anterior to the caudal region of the cell" [66].

The importance of microtubule motors and microtubule-dependent transport in testes is suggested by the following observations: 1) Sertoli cells contain ordered, parallel arrays of microtubules (associated with membranous organelles) with their [−] ends extending towards the seminiferous tubule lumen [20]; 2) microtubules are situated around germ cell-associated ectoplasmic specializations while the germ cells are translocated through the seminiferous epithelium [20, 51]; 3) manchettes are microtubule structures that contain cross-linking proteins and are associated with cytoplasmic vesicles [51, 66, 68]; and 4) rat testis and Sertoli cells are a rich source of cytoplasmic dynein [31, 44, 45]. The aim of the experiments described here was to immunolocalize kinesin and cytoplasmic dynein within rat testis in order to elaborate the possible roles of these microtubule motors in spermatogenesis.

MATERIALS AND METHODS

General

Adult (200–250 g) Sprague Dawley CD (Charles River Breeding Labs., Wilmington, MA) rats were housed at 22 ± 1°C under a 12 L:12 D cycle with 35–70% humidity in wire cages with ad libitum food and water. SDS-PAGE [69] was performed using rabbit muscle myosin (205 kDa), β-galactosidase (116 kDa), BSA (66 kDa), and ovalbumin (44 kDa) as molecular mass standards and the Phastsystem gel apparatus (Pharmacia LKB Biotechnology, Inc., Piscataway, NJ). Pre-cast gels (7.5% or 4–15%) were either silver-stained [70] or electroblotted onto nitrocellulose using the Phast-Transfer apparatus (Pharmacia LKB Biotechnology, Inc.). For immunohistochemistry, testes were removed from CO_2-asphyxiated rats and immediately frozen in embedding medium (O.C.T. Compound, Miles, Inc., Elkhart, IN) in liquid nitrogen. The frozen blocks were stored at −80°C until sectioned. Testes were sectioned at 8 μm, thawed onto poly-L-lysine-coated slides, dried, and fixed appropriately. Unless otherwise noted, all chemicals were obtained from Sigma Chemical Co. (St. Louis, MO).Photographs were taken using Tri-X Pan, Technical Pan 4125, or Ecktachrome-400 (Kodak, Rochester, NY) film using Zeiss Axioplan or Zeiss Axiovert microscopes equipped with epifluorescence and filters for fluorescein (excitation: 450–490; barrier: 510; emission: 515–556), rhodamine (excitation: 546; barrier: 580; emission: 590) and *bis*-benzimide (excitation: 365; barrier: 395; emission: 420).

Preparation of Cytoplasmic Dynein and Kinesin

To prepare a crude cytoplasmic dynein fraction, testes were removed from CO_2-asphyxiated adult rats and homogenized in 0.1 M 2-[N-morpholino]ethane-sulfonic acid, 0.5 mM $MgCl_2$, 1 mM EGTA, 4 M glycerol, 0.2 mM PMSF, pH 6.75 (MES buffer); 4.2 μM leupeptin; and 0.1 mg/ml soybean trypsin inhibitor [44, 46]. The homogenate was centrifuged for 45 min at 100 000 × *g* at 4°C. The pellet was discarded, and the supernatant was centrifuged for 45 min at 125 000 × *g* at 4°C. Taxol (kindly provided by Dr. Nancita R. Lomax, National Cancer Institute, Bethesda, MD) was added to the supernatant to 20 μM, and microtubules were allowed to polymerize for 10 min at 37°C and 20 min at 4°C. The microtubules were sedimented through a 25% sucrose plus 20 μM taxol cushion for 30 min at 100 000 × *g* at 4°C. The resulting pellet was resuspended in MES buffer plus 20 μM taxol and gently homogenized. The homogenate was cooled on ice for 5 min and centrifuged for 30 min at 80 000 × *g* at 4°C. The pellet was gently homogenized in MES buffer with 5 mM guanosine triphosphate (GTP)

and 5 mM $MgCl_2$, and incubated at room temperature for 15 min and at 37°C for 10 min. This mixture was centrifuged for 30 min at 80 000 × *g* at 29°C; the pellet was gently homogenized in MES buffer with 5 mM ATP and 5 mM $MgCl_2$ and then incubated at room temperature for 15 min and 37°C for 10 min to release microtubule-associated proteins, including cytoplasmic dynein. This protein mixture was centrifuged for 30 min at 80 000 × *g* at 29°C, and the supernatant was taken as the crude cytoplasmic dynein preparation.

Kinesin was prepared from bovine brain [71]. One hundred forty grams of fresh bovine brain white matter and brain stem were homogenized in PME buffer (PIPES, 5 mM $MgSO_4$, 1 mM EGTA, pH 6.9) with protease inhibitors (1 μg/ml leupeptin, 10 μg/ml soybean trypsin inhibitor, and 0.2 mM PMSF). The homogenate was centrifuged at 30 000 × *g* for 45 min at 4°C, and the supernatant was frozen until used. After thawing, 90 ml of crude supernatant was brought up to 20 μM taxol and 1 mM GTP and warmed to 25°C for 30 min. ATP was added to bring the solution up to 0.1 mM, and the mixture was centrifuged at 120 000 × *g* for 45 min at 25°C. Kinesin was purified from the microtubule-depleted supernatant by adding pure bovine brain tubulin at 0.25 mg/ml to 10 mg/ml D-glucose, 18 U/ml hexokinase, 0.4 mM 5′-adenylylimidodiphosphate (AMP-PNP) with 10 μM taxol, and incubation at 25°C for 30 min. This mixture was then centrifuged through a 20% (wt/vol) sucrose cushion in PMED (PME buffer plus 2 mM dithiothreitol) at 150 000 × *g* for 45 min at 25°C. The resulting pellet was resuspended in 20 volumes of PMED with 10 μM taxol and 0.1 mM AMP-PNP and centrifuged through a 20% sucrose cushion (plus 10 μM taxol, 0.1 mM AMP-PNP) at 150 000 × *g* for 45 min at 25°C. The pellet was resuspended in 20 volumes of PMED plus 10 mM ATP and 0.3 M NaCl and centrifuged through another 20% sucrose cushion (plus 6.7 mM ATP, 0.3 M NaCl) at 150 000 × *g* for 45 min at 25°C. The supernatant fraction collected above the cushion was concentrated using an ultrafiltration cell (Amicon Corp., Lexington, MA) with a P30 membrane. The concentrated supernatant was further purified on a 5–20% sucrose gradient that was centrifuged overnight in a Beckman (Palo Alto, CA) SW40Ti rotor at 100 000 × *g* at 4°C. Fractions of 0.4 ml were collected from the bottom of the gradient, and fractions 8 and 9 were combined as the kinesin fraction as determined by SDS-PAGE.

Antibodies

A mouse monoclonal antibody (IgM) raised against intermediate chains of chick brain cytoplasmic dynein (clone 70.1) [29] was obtained from Michael Sheetz (Duke University Medical Center, Durham, NC) and mouse monoclonal antibodies (IgG) against bovine brain kinesin heavy chains (clones H1 and H2) [72] were obtained from Scott Brady (University of Texas Southwestern Medical Center, Dallas, TX). To verify the specificity of the antibodies, crude

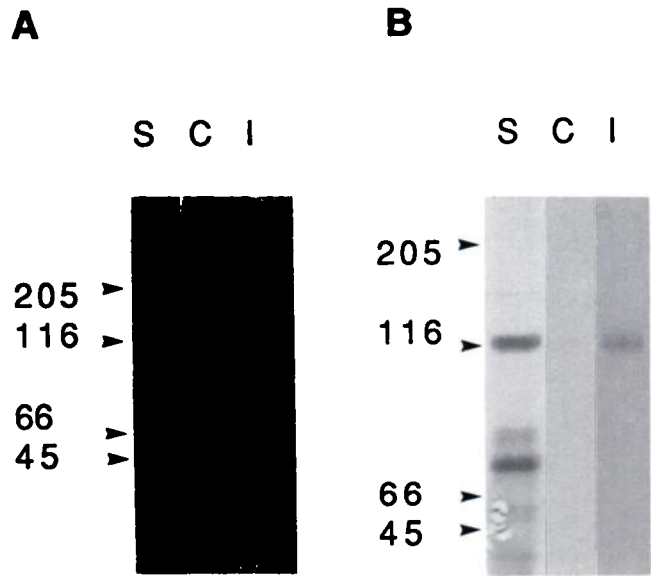

FIG. 1. A) SDS-PAGE gel (4–15% gradient) of crude rat testis cytoplasmic dynein. Lane S: Silver-stained gel. Lane C: Control immunoblot without first antibody. Lane I: Immunoblot stained for cytoplasmic dynein intermediate chain revealing a single band at 72 kDa. B) SDS-PAGE gel (7.5%) of bovine brain kinesin. Lane S: Silver-stained gel. Lane C: Control immunoblot. Lane I: Immunoblot stained for kinesin heavy chain revealing a single band at 115 kDa. Positions of molecular mass standards are indicated to the left.

cytoplasmic dynein and kinesin preparations were separated by SDS-PAGE [69] and then electroblotted onto nitrocellulose. Immunoreactive bands were detected by means of biotinylated horse anti-mouse IgG (Vector Laboratories, Burlingame, CA) or biotinylated goat anti-mouse IgM (Organon Teknika Corporation, Durham, NC) followed by peroxidase-conjugated avidin-biotin complex (Vectastain ABC, Vector Laboratories) and reaction with 0.09% H_2O_2 and 0.25 mg/ml diaminobenzidene. Nonspecific binding was blocked using 0.5% gelatin prior to application of primary antibodies.

The cytoplasmic dynein antibody reacted with a single band of 72 kDa in immunoblots of rat testis cytoplasmic dynein crude preparations (Fig. 1A), whereas the H1 kinesin antibody produced a single band of 115 kDa on immunoblots of bovine brain kinesin (Fig. 1B). These molecular sizes are within published ranges for these proteins [25, 46, 73, 74]. Omitting the first antibodies or replacing them with normal mouse IgG or an irrelevant monoclonal IgM (HNK-1, kindly provided by Ken Reuhl, Rutgers College of Pharmacy, Piscataway, NJ) eliminated the fluorescence produced with the anti-kinesin or anti-cytoplasmic dynein antibodies, respectively. Finally, overnight preabsorption of these antibodies with excess bovine brain kinesin or rat testis cytoplasmic dynein blocked their binding to rat testis frozen sections (data not shown).

Cytoplasmic Dynein and Kinesin Immunohistochemistry

After drying, testis cross sections were fixed with 0.5% paraformaldehyde in PBS for 10 min and −20°C methanol

for 10 min. The slides were allowed to dry briefly, and nonspecific binding was blocked by a 5-min incubation with 1–5% normal goat serum, 1% BSA in PBS. Anti-cytoplasmic dynein (40.0 μg/ml) or anti-kinesin (17.5 μg/ml) antibodies were applied to each section for 1–2 h at room temperature in a humidified chamber. The slides were rinsed in PBS (once briefly for the anti-cytoplasmic dynein and three times for 5 min each for the anti-kinesin), and incubated for 1 h with fluorescein-conjugated goat anti-mouse IgM (Fisher Biotech, Medford, MA) diluted 1:100 or fluorescein-conjugated goat anti-mouse IgG (Fisher Biotech) diluted 1:400 in blocking solution. After rinsing, the sections were coverslipped using 0.1% paraphenylydiamine in 50% glycerol.

For triple labeling, testis cross sections were fixed for 10 min with 0.5% paraformaldehyde followed by 5 min in −20°C acetone. After drying, actin was fluorescently labeled by incubating the sections with 0.5 μg/ml tetramethylrhodamine B isothiocyanate (TRITC)-conjugated phalloidin in PBS for 20 min. This was followed by −20°C MeOH for 5 min and cytoplasmic dynein immunostaining as described above. Prior to coverslipping, 0.2 μg/ml *bis*-benzimide was added to the slides for 2 min to fluorescently label cell nuclei. The slides were then rinsed and coverslipped as described above. Staging of seminiferous tubules using standard criteria [10] was accomplished using a combination of differential interference contrast (DIC) microscopy and *bis*-benzimide fluorescence.

Manchette Isolation and Immunofluorescence

Manchette-enriched preparations were obtained from adult rat testes by mincing decapsulated testes in homogenization buffer (0.1 M PBS plus 1% Triton X-100, 1 mM $MgCl_2$, 0.4 mg/ml DNase I, 0.5 mM PMSF, 10 μg/ml soybean trypsin inhibitor, 0.5 μg/ml pepstatin, 0.5 μg/ml leupeptin, 10 mg/ml D[+]-glucose, 18 U/ml hexokinase, and 0.4 mM AMP-PNP). The minced testes were filtered through a 70-μm Nitex nylon screen (Tetko, Briarcliff, NY) and centrifuged at 1 000 × *g* for 10 min at 20°C. The resulting pellet was gently resuspended in PBS with 0.4 mM AMP-PNP and centrifuged at 13 000 × *g* in a microcentrifuge for 5 min at 4°C. The pellet was washed twice with PBS plus 0.4 mM AMP-PNP. The final pellet was resuspended in 100 μl PBS plus 0.4 mM AMP-PNP, and 5-μl aliquots were dried onto microscope slides. The dried slides were fixed for 10 min with 0.5% paraformaldehyde in PBS followed by −20°C MeOH for 10 min. Blocking solution was applied to the slides for 5–10 min; then mixtures of either anti-cytoplasmic dynein (0.04 mg/ml, clone 70.1) and rabbit anti-tubulin (Sigma; diluted 1:20) or anti-kinesin (17.5 μg/ml, clone H1 + H2) and mouse IgM anti-tubulin (BIOPRODUCTS for Science, Indianapolis, IN; clone T1–10; diluted 1:5) antibodies were applied to the slides for 1 h. Although clones H1 and H2 anti-kinesin antibodies produced identical results, a mixture of the antibodies yielded a darker band on the immunoblot; thus a combination of the two antibodies was used. After the slides were rinsed in PBS, fluorescein isothiocyanate (FITC)-conjugated goat anti-mouse IgM and TRITC-conjugated goat anti-rabbit IgG antibodies were applied to the cytoplasmic dynein antibody-exposed slides, and FITC-conjugated goat anti-mouse IgG and TRITC-conjugated goat anti-mouse IgM antibodies were applied to the anti-kinesin-exposed slides for 1 h at room temperature in a dark, humid chamber. After rinsing in PBS, the slides were coverslipped with 0.1% paraphenyldiamine in 50% glycerol in PBS.

Rat cytoplasmic dynein and kinesin were purified from a manchette-enriched preparation isolated from 25 adult rats using a modification of the procedure described above. After centrigugation at 1 000 × *g*, the pellet was resuspended in 0.1 M PME buffer with 0.4 mM AMP-PNP. This suspension was centrifuged at 13 000 × *g* for 5 min at 4°C, and the pellet was washed three times in PIPES buffer with 0.4 mM AMP-PNP. After the final wash, the pellet was incubated with 10 mM ATP, 10 mM Mg^{2+} in PIPES buffer for 10 min at 20°C to release cytoplasmic dynein and kinesin from microtubules. After centrifuging at 100 000 × *g* for 10 min in a Beckman Airfuge, the 1.0-ml supernatant was loaded onto an 11.0-ml 5–20% sucrose gradient in PIPES buffer and centrifuged at 100 000 × *g* for 18 h at 4°C in a Beckman SW40Ti rotor. Fractions (500 μl) were collected from the gradient and separated by SDS-PAGE. Fractions 8 and 15 were taken as the cytoplasmic dynein and kinesin preparations, respectively. These fractions were separated by SDS-PAGE and electroblotted onto nitrocellulose for immunoblotting. The fraction 8 lane was immunostained with anti-cytoplasmic dynein as previously described, while the fraction 15 lane was immunostained with a mixture of clone H1 and clone H2 anti-kinesin heavy-chain antibodies. Although clone H1 produced a visible band in the same location, we found that a mixture of clones H1 and H2 produced a stronger signal.

RESULTS

Cytoplasmic Dynein Immunohistochemistry

Antibodies raised against cytoplasmic dynein revealed immunoreactivity in the interstitium and seminiferous tubules. The interstitial staining was localized to the cytoplasm of Leydig cells and occurred in a diffuse, granular pattern. The seminiferous epithelial staining was most obvious in Sertoli cell cytoplasm as diffuse fluorescence at all stages of the seminiferous epithelial cycle leaving a negatively stained image of germ cells and Sertoli cell nuclei (Fig. 2). Intensely staining germ cell-associated ectoplasmic specializations, manchettes, and germ cell cytoplasmic structures were visible in a stage-dependent pattern.

In seminiferous tubules of stages I-IV, spermatid manchettes were immunoreactive with the cytoplasmic dynein antibody (Fig. 2, a and b). The cytoplasmic dynein immu-

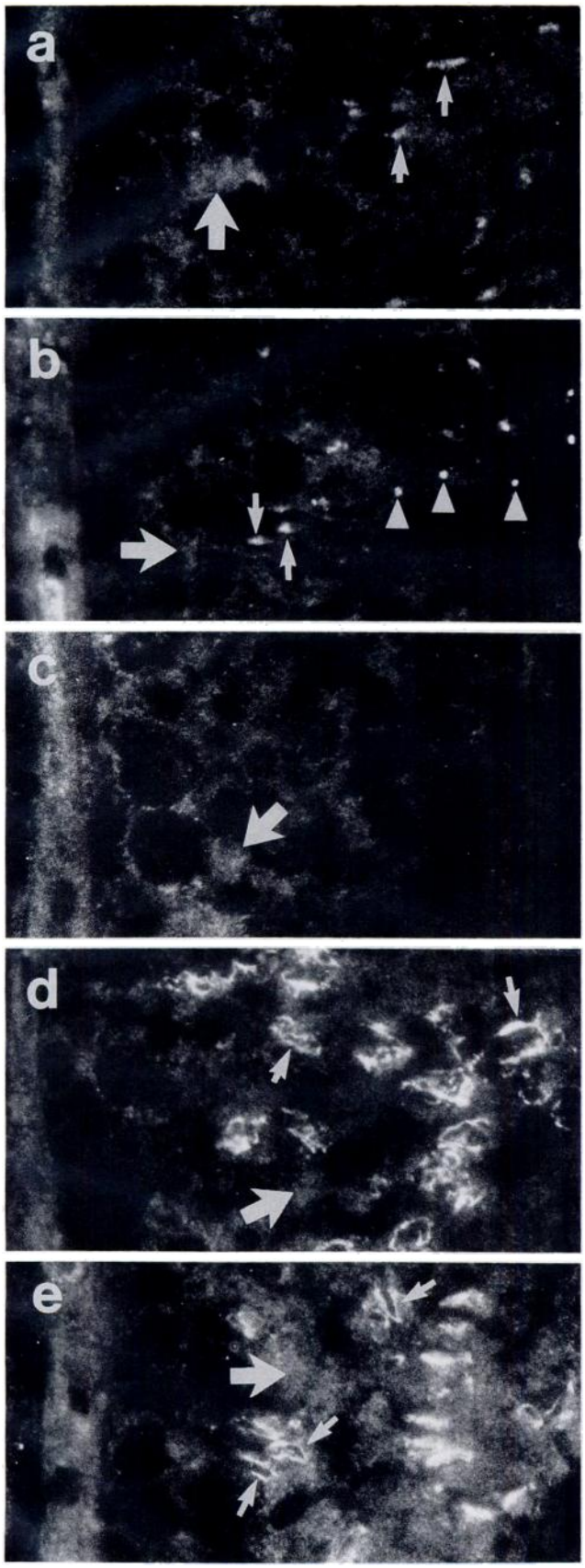

FIG. 2. Immunolocalization of cytoplasmic dynein in rat testis cross sections. a) Stage I-III tubule exhibits Sertoli cell cytoplasmic (large arrow) and manchette (small arrows) staining. b) Stage IV tubule exhibits circular staining in spermatid cytoplasm (arrowheads) in addition to the Sertoli cell cytoplasmic (large arrow) and manchette staining (small arrows). c) This stage VII-VIII tubule exhibits only the Sertoli cell cytoplasmic staining (large arrow). d) Stage IX-X tubule exhibits more intense Sertoli cell cytoplasmic staining (large arrow) as well as staining in the ectoplasmic specialization regions of step 9 and 10 spermatids (small arrows). e) Stage XI-XIV tubule exhibits the most intense Sertoli cell cytoplasmic staining (large arrow) in addition to the ectoplasmic specialization staining (small arrows). ×720.

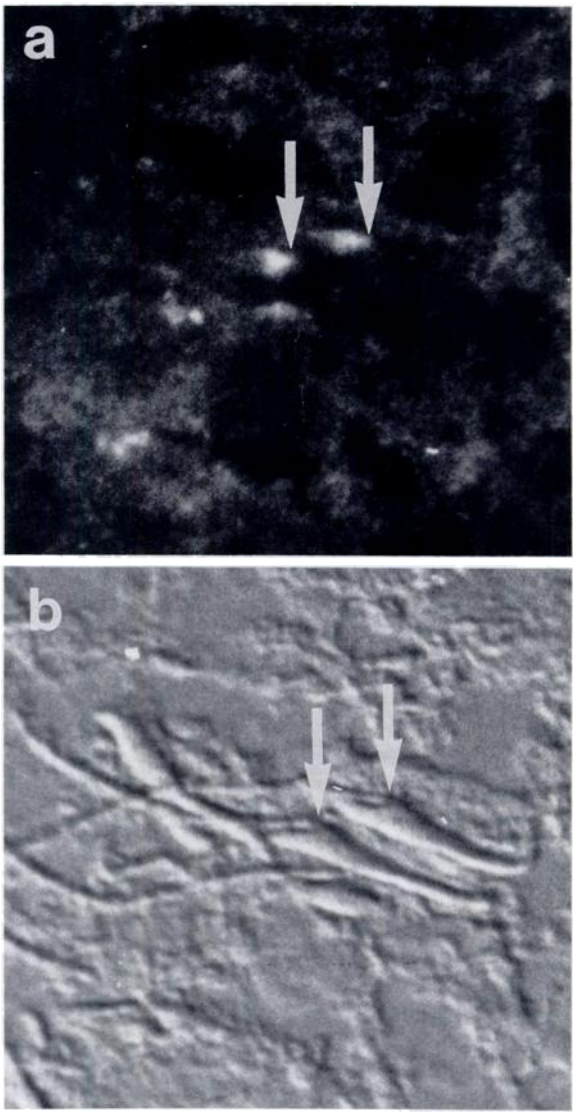

FIG. 3. Cytoplasmic dynein immunofluorescence in rat testis manchettes. a) Cytoplasmic dynein immunofluorescence associated with the ventral aspect of the caudal head of step 17 (stage IV) spermatids (arrows). b) DIC photomicrograph of the same spermatids (arrows). ×1 890.

noreactive manchette structures appeared as short, linear projections associated with the ventral aspect of the caudal head of the elongate spermatid (Fig. 3). In stage V-VI tubules, small (~1.5 μm), round, hollow structures in the cytoplasm of elongate spermatids exhibited cytoplasmic dynein immunofluorescence (Fig. 2b). To verify that these structures were not associated with germ cell Golgi apparatus, sections were stained with the anti-cytoplasmic dynein antibody and with TRITC-conjugated wheat germ agglutinin [75] or N-[7-(4-nitrobenzo-2-oxa-1,3-diazole)]-6-aminocaproyl sphingosine (C6-NBD-ceramide) [76] (data not shown). In both cases, the Golgi apparatus were readily apparent and separate from the cytoplasmic dynein staining. In stage V tubules, the spermatid cytoplasmic structures and Sertoli cell cytoplasmic staining remained, whereas the manchette staining was no longer present (data not shown). In stage VIII tubules, only the Sertoli cell cytoplasmic immunofluorescence was evident (Fig. 2c).

During stages IX-XIV, apical regions of Sertoli cell cytoplasm were most intensely stained, and staining was also evident around the spermatids (Fig. 2, d and e). This ectoplasmic-specialization region staining was limited to step 9–14 spermatids. To verify that the staining was not in the germ cell cytoplasm, testis cross sections were immunostained for cytoplasmic dynein and then counterstained with the nuclear florescent dye *bis*-benzimide. This demonstrated that the cytoplasmic dynein was present in Sertoli cell cytoplasm and probably not germ cell cytoplasm (Fig. 4a). Since ectoplasmic specializations are actin-rich structures, sections were stained with anti-cytoplasmic dynein antibody, *bis*-benzimide, and TRITC-phalloidin (specific for filamentous actin; Fig. 4b). The resulting orange-red TRITC-phalloidin fluorescence almost completely obscured the green FITC-cytoplasmic dynein immunofluorescence, indicating the co-localization of cytoplasmic dynein immunoreactivity with the actin-rich ectoplasmic specializations.

Kinesin Immunohistochemistry

Immunofluorescent staining of testis cross sections with a monoclonal antibody against the heavy chain of bovine brain kinesin revealed very faint staining of the interstitium and intense, stage-dependent staining within the seminiferous epithelium (Fig. 5). This intense immunoreactivity was associated with manchettes of elongate spermatids. The localization of kinesin immunoreactivity to manchettes was determined by the immunofluorescent appearance, co-localization with tubulin immunoreactivity (data not shown), and cytoplasmic relationship to the spermatid nucleus as determined using DIC microscopy (Fig. 6) and *bis*-benzimide fluorescence (data not shown). Step 10–14 spermatids exhibited manchettes extending from the posterior aspect of the spermatid nuclei (Fig. 5d), while step 15–18 spermatids exhibited an intensely staining linear manchette that trailed from the posterior aspect of the spermatid nucleus (Fig. 5, a and b). Kinesin immunoreactivity in stages IV-V (Fig. 5b) and stage VI (Fig. 5c) also presented a punctate appearance in spermatid cytoplasm. No kinesin immunoreactivity was evident in stages VII-IX. In contrast to the cytoplasmic dynein immunoreactive structures in the spermatid cytoplasm, the kinesin immunoreactive structures often co-localized with tubulin immunofluorescence (data not shown); they were more variable in size (0.5–1.0 μm), they were solid, and they did not co-localize with cytoplasmic dynein (data not shown).

FIG. 4. Testis cross sections fluorescently labeled with anti-cytoplasmic dynein, TRITC-phalloidin, and *bis*-benzimide. a) Stage XI-XII tubule demonstrates the localization of the cytoplasmic dynein immunoreactivity (green) to the ectoplasmic specialization regions of elongate spermatids (small arrows). The lack of germ cell cytoplasmic staining is evident as a negatively stained space between the germ cell nucleus (blue) and the cytoplasmic or ectoplasmic specialization staining (arrowheads). b) Stage X tubule stained with TRITC-conjugated phalloidin, anti-cytoplasmic dynein, and *bis*-benzimide demonstrates the co-localization of the ectoplasmic specialization region cytoplasmic dynein staining with actin (red-orange). The red-orange actin fluorescence co-localizes with the green cytoplasmic dynein immunofluorescence (arrow). ×1 200.

Manchette Immunofluorescence

To verify the immunolocalization of cytoplasmic dynein and kinesin to manchettes, manchette-enriched preparations were double-labeled with anti-cytoplasmic dynein (IgM) and rabbit anti-tubulin (IgG), or anti-kinesin (IgG) and mouse anti-tubulin (IgM). Anti-cytoplasmic dynein (Fig. 7a) and anti-kinesin (Fig. 8a) immunofluorescence co-localized with anti-tubulin immunofluorescence (Figs. 7b and 8b) to structures with the characteristic morphology of manchettes (Figs. 7c and 8c); thus the immunoreactive kinesin and cytoplasmic dynein were found in the tubulin-rich manchettes. When stained with the mouse anti-tubulin (IgM), nuclear rings were revealed as brightly stained lines at the base of the manchettes (Fig. 8b).

The observed cytoplasmic dynein and kinesin immunoreactivity in manchettes provided an opportunity to verify that the manchette cytoplasmic dynein and kinesin immunoreactivity was associated with microtubule motors. Crude preparations of manchettes were isolated in ATP-depleting conditions in the presence of AMP-PNP to determine biochemically if those structures contained the bound microtubule motors cytoplasmic dynein and kinesin. Microtubule motors were released from the manchettes with 10 mM Mg^{2+} ATP and then separated on a 5–20% sucrose gradient. The gradient was then fractionated, and the fractions were analyzed by SDS-PAGE (Fig. 9A). High molecular mass bands in fractions 6–9 were evident, consistent with previously reported isolations of rat testicular cytoplasmic dynein [44, 45]. Bands in fractions 13–16 were consistent in appearance with those previously reported for purified bovine brain kinesin [72]. The presence of these microtubule motors in crude manchette ATP eluates was confirmed by immunoblotting of the appropriate fractions (Fig. 9B). Frac-

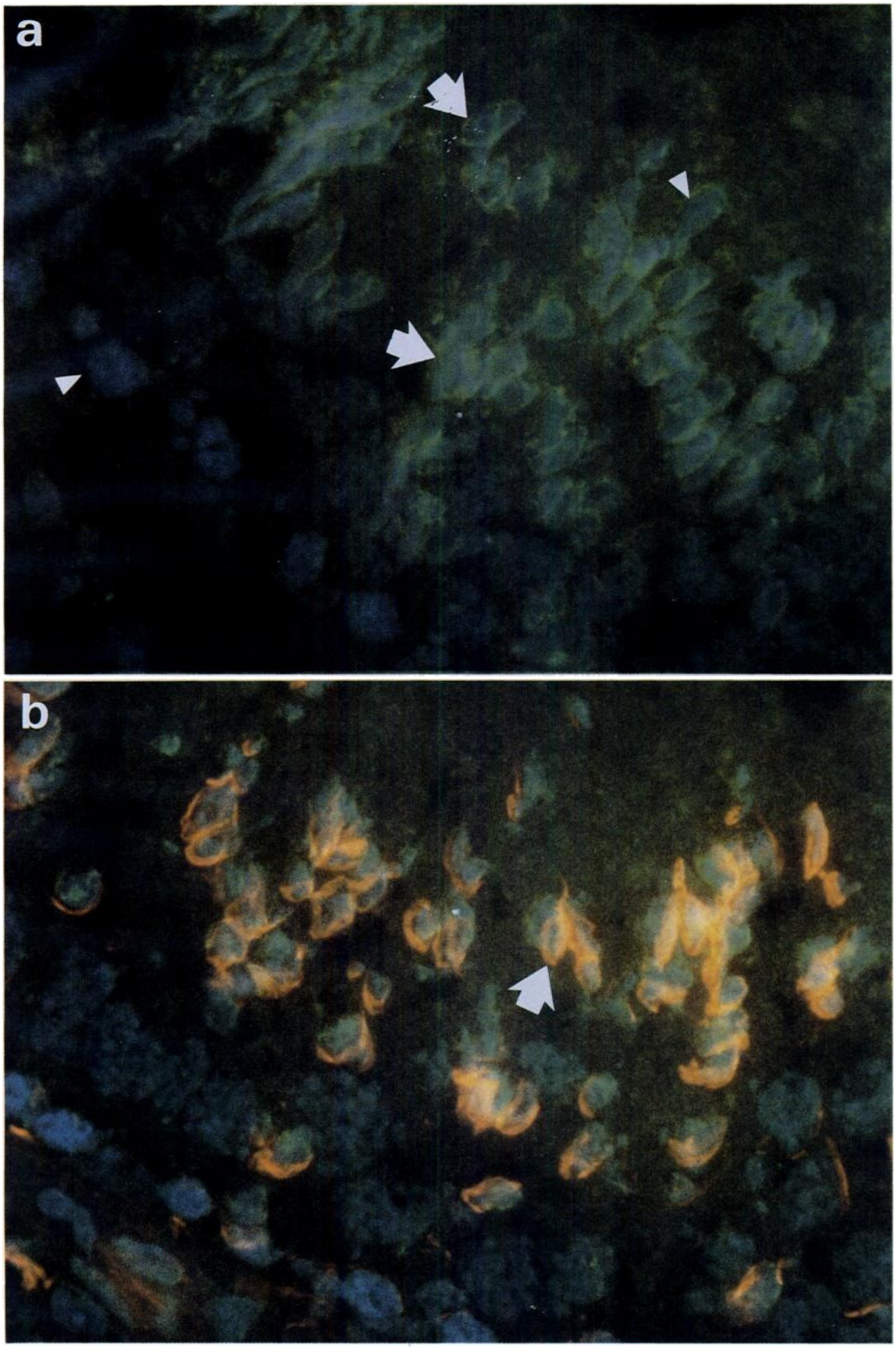

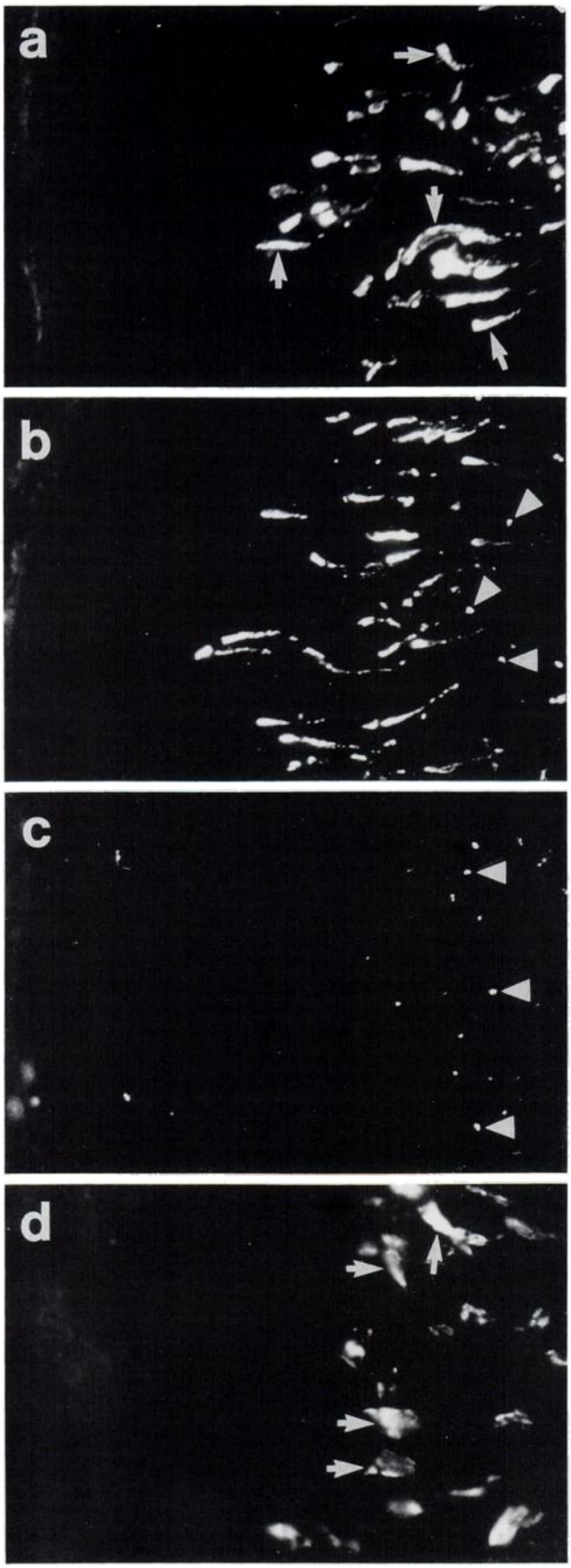

FIG. 5. Kinesin immunohistochemistry. a) Stage I-IV tubule exhibits linear manchette staining (small arrows). b) Stage V tubule reveals the appearance of punctate staining within spermatid cytoplasm (arrowheads). c) When manchettes are being disassembled in stage VI, the kinesin immunofluorescence is limited to punctate staining in spermatid cytoplasm (arrowheads). d) Stage XI-XIII tubule exhibits manchette staining (small arrows). The basement membrane of each tubule is located at the left edge of each photograph. ×720.

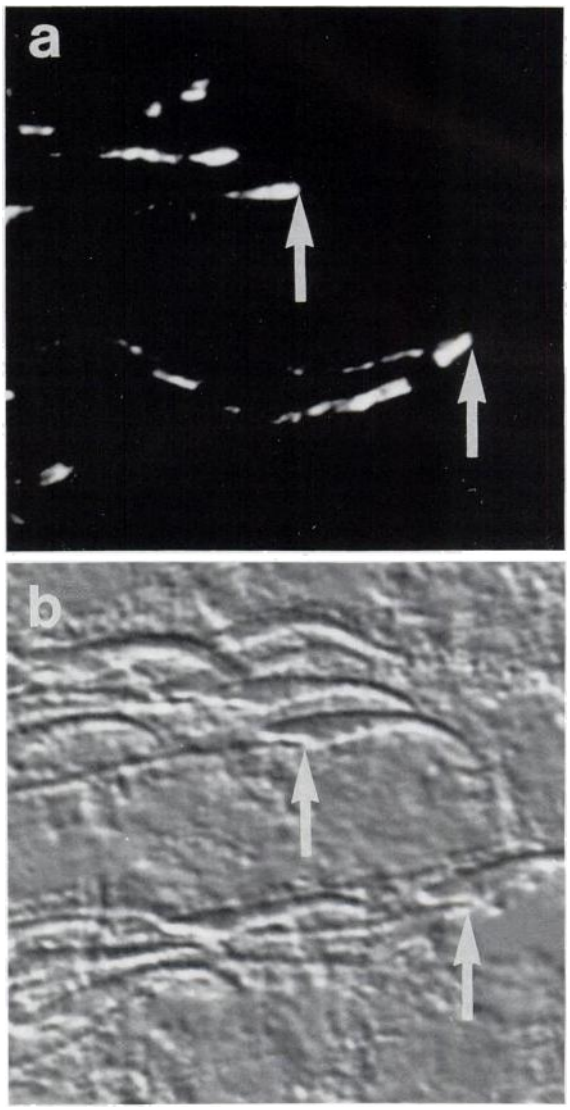

FIG. 6. Kinesin immunofluorescence in rat testis manchettes. a) Kinesin immunofluorescence associated with the ventral aspect of the caudal head of step 17 (stage V) spermatid nuclei (arrows). b) DIC photomicrograph of the same spermatids (arrows). ×1 890.

tion 8 was immunostained with anti-cytoplasmic dynein intermediate chain, resulting in an immunoreactive band at 74 kDa. Fraction 15 was immunostained with anti-kinesin heavy chain, producing a single band at 110 kDa.

DISCUSSION

Sertoli cells provide the necessary physical and biochemical environment for spermatogenesis. They form the

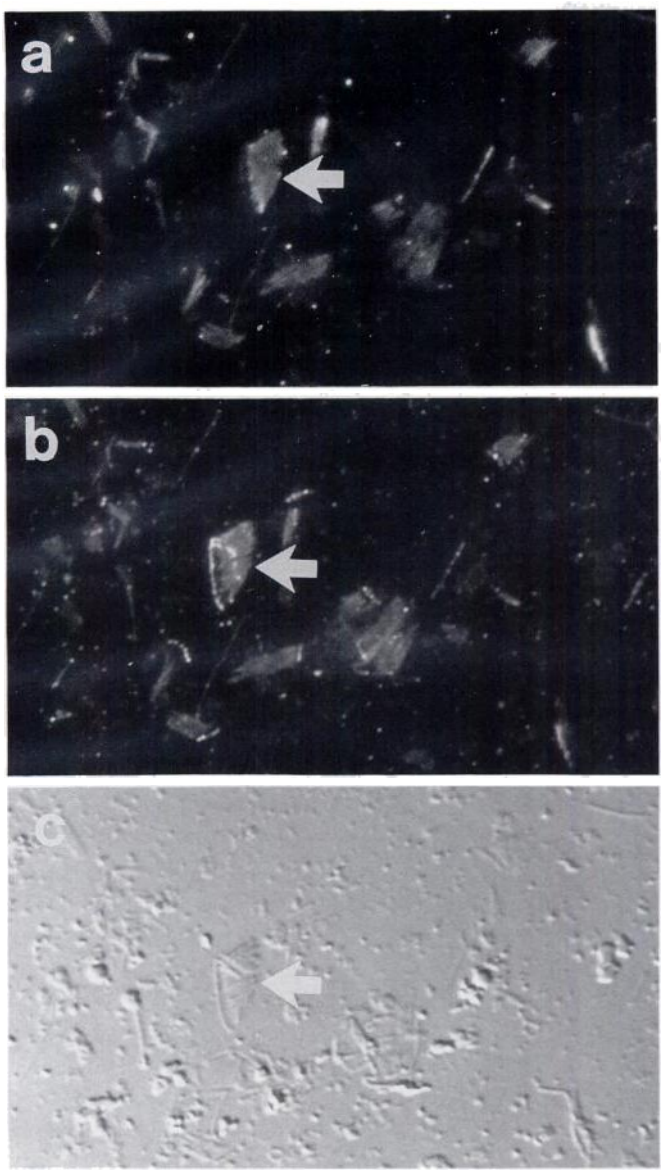

FIG. 7. Double immunofluorescent labeling of a manchette-enriched preparation with anti-cytoplasmic dynein and anti-tubulin antibodies. a) Manchette immunostained with the anti-cytoplasmic dynein antibody (arrow). b) Same manchette immunostained with an anti-tubulin antibody (arrow). c) DIC image of the same manchette (arrow). ×1 150.

blood-testis barrier, isolating germ cells in the adluminal compartment from interstitial fluids. Sertoli cells are probably responsible for translocating germ cells through the seminiferous epithelium, and they embrace maturing germ cells within crypts that accommodate the changing shapes of spermatids. Sertoli cells provide an ideal biochemical environment through the selective secretion of materials (either transported from the interstitium or synthesized) into the space surrounding the germ cells. The possible involvement of microtubule-dependent mechanoenzymes in these processes was explored by studying the immunodistribution of cytoplasmic dynein and kinesin within rat testis.

Immunoreactive cytoplasmic dynein and kinesin were detected in rat testes with a stage-dependent distribution (Fig. 10). Cytoplasmic dynein was immunolocalized to Sertoli cell cytoplasm during all stages of spermatogenesis; however, apical Sertoli cell cytoplasm exhibited its most intense immunofluorescence during stages IX-XIV (Fig. 2). Since Sertoli cell microtubules are oriented with their [−] ends towards the seminiferous tubule lumen [20] and cytoplasmic dynein is a [−] end-directed motor [23], the stage-dependent cytoplasmic dynein staining is probably a manifestation of stage-dependent microtubule-based transport processes. This hypothesis is supported by the secretion of

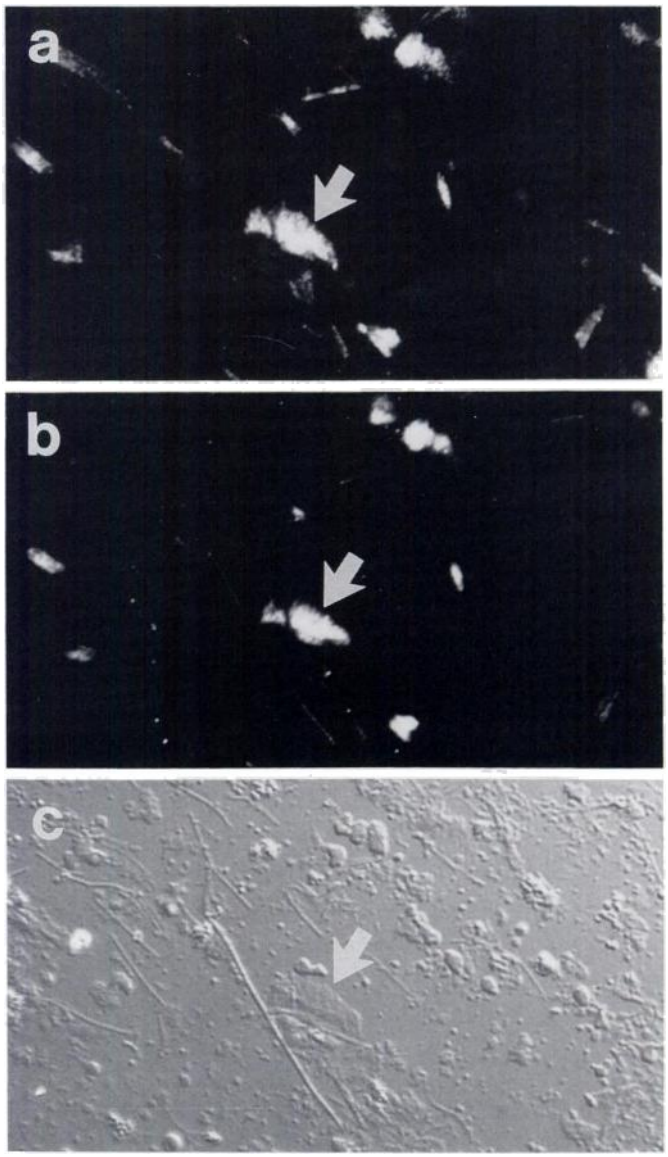

FIG. 8. Double immunofluorescent labeling of a manchette-enriched preparation with anti-kinesin and anti-tubulin antibodies. a) Manchette immunostained with the anti-kinesin antibody (arrow). b) Same manchette immunostained with an anti-tubulin antibody (arrow). c) DIC image of the same manchette (arrow). ×1 150.

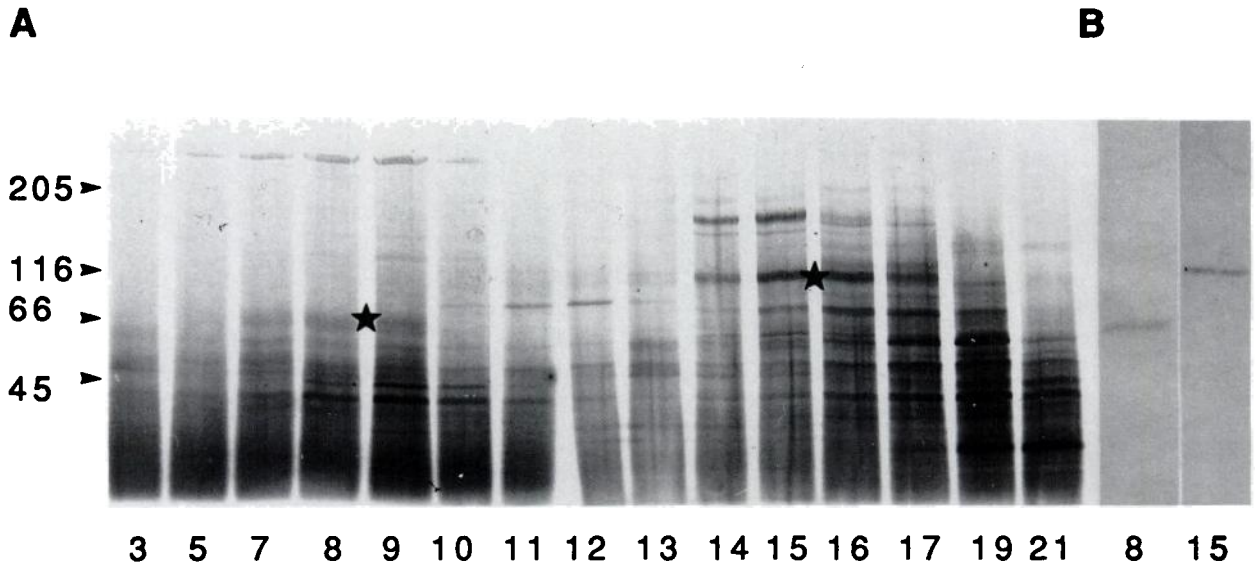

FIG. 9. A) Silver-stained 4–15% gel of fractions collected from the bottom of a 5–20% sucrose gradient separation of manchette microtubule-associated proteins. Fraction numbers are listed along the bottom of the figure. Molecular mass standards are indicated along the left side. Fractions 8 and 15 were collected as the cytoplasmic dynein (star) and kinesin (star) fractions, respectively. B) Immunoblots of fractions 8 and 15 stained with clone 70.1 anti-intermediate chain cytoplasmic dynein or clone H1 + H2 anti-heavy chain kinesin, respectively. Fraction 8 reveals a single cytoplasmic dynein immunoreactive band of 74 kDa, and fraction 15 produces a single kinesin immunoreactive band of 110 kDa.

androgen-binding protein and transferrin, which are highest during stages VIII-XII [11].

Cytoplasmic dynein immunofluorescence was also evident in the ectoplasmic specializations of step 9–14 spermatids. There are four explanations for the possible function of cytoplasmic dynein in ectoplasmic specializations. First, ectoplasmic specializations may be involved in the positioning and translocation of spermatids during spermatogenesis [20, 51–54]. Second, an accumulation of cytoplasmic dynein near ectoplasmic specializations may represent the termini for cytoplasmic dynein-based transport and secretion. Third, cytoplasmic dynein-based transport may be involved in ectoplasmic specialization formation. Fourth, the association of a force-exerting mechanoenzyme in this location suggests a possible role in spermatid reshaping.

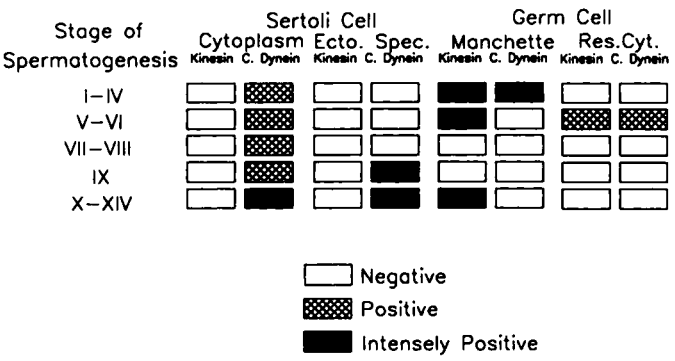

FIG. 10. Summary of the stage-dependent immunolocalization of cytoplasmic dynein and kinesin within rat testes.

The first hypothesis proposes that microtubule motors (possibly cytoplasmic dynein) bind to the endoplasmic reticulum of spermatid-associated ectoplasmic specializations, re-orient elongate germ cells, and move the Sertoli cell crypts, spermatids, and ectoplasmic specializations along the oriented microtubules of the Sertoli cell [20, 51, 52]. Cytoplasmic dynein immunoreactive to clone 70.1 (anti-intermediate chain cytoplasmic dynein) is probably not involved in ectoplasmic specialization-dependent spermatid translocation because cytoplasmic dynein immunofluorescent staining of ectoplasmic specializations was observed during stages IX-XIV, and the period of greatest excursion of the spermatids within the seminiferous epithelium is observed during stages IV-VI [10].

The second hypothesis contends that cytoplasmic dynein accumulates at the termini for Sertoli cell transport and secretion. This is supported by the observation that peak apical cytoplasmic dynein immunofluorescence coincided with peak periods of Sertoli cell secretion of androgen-binding protein and transferrin [11]; however, secretion through the dense actin networks lying between cytoplasmic microtubules, smooth endoplasmic reticulum, and the Sertoli cell membrane seems unlikely.

The third hypothesis proposes that cytoplasmic dynein-mediated transport is involved in delivering materials necessary for the formation of ectoplasmic specializations. This is supported by the appearance of ectoplasmic specialization immunoreactivity when the ectoplasmic specializations are forming.

A fourth hypothesis suggests that cytoplasmic dynein is involved in the complex morphological changes that occur

during stages IX-XIV when round spermatids begin to flatten and elongate. An association between a force-exerting microtubule motor and ectoplasmic specializations during this time suggests that ectoplasmic specializations may be involved in spermatid reshaping. The intermediate filaments extending from the Sertoli cell crypts to the base of the cell may act as anchors [77]; thus, cytoplasmic dynein bound to the smooth endoplasmic reticulum of the spermatid-associated ectoplasmic specialization and neighboring microtubules may exert a lumenally directed force along the walls of the crypt that might squeeze spermatid cytoplasm towards the seminiferous tubule lumen and compress the anterior aspect of the spermatid nucleus.

Manchettes are formed by a cylinder of microtubules and microtubule-associated proteins that extends from the posterior of the spermatid towards the tubule lumen. Electron microscopy has demonstrated manchette microtubules crosslinked to the nuclear membrane, endoplasmic reticulum, and cytoplasmic vesicles [52, 65, 66, 68]. The connections with the nuclear membrane support the hypothesis that manchettes are involved in spermatid nuclear reshaping [65], while the association with cytoplasmic vesicles has led to the hypothesis that they are involved in vesicle transport [66, 68]. Conceptually, both of these hypotheses are supported by the immunolocalization of cytoplasmic dynein and kinesin to manchettes. The orientation of microtubules within manchettes is not known; however, since cytoplasmic dynein is [−] end-directed and kinesin is [+] end-directed, transport along manchettes is probably bidirectional.

The cytoplasmic dynein immunoreactivity within manchettes of steps 15–17 (stages I-IV) spermatids (Fig. 2, a and b) suggests that cytoplasmic dynein-dependent processes occur along manchettes only during spermatogenic stages I-IV. On the other hand, kinesin was detected in manchettes beginning with their first appearance in stage X and ending with their disassembly in stage VI. Thus, kinesin-dependent manchette processes may be important during a much longer period of spermatid maturation.

The cytoplasmic dynein immunoreactive structures in the spermatid cytoplasm appeared as small (~1.5 μm) hollow circles. They appeared in stage V-VI tubules, coincident with disassembly of manchettes. This association suggests that these structures are involved in manchette disassembly or some other process occurring in the spermatid cytoplasm. Immunoelectron microscopy will be necessary to further define the location and morphology of these structures. Kinesin was also immunolocalized to cytoplasm of steps 17 and 18 (stage V-VI) spermatids. The spermatid cytoplasmic kinesin immunoreactivity presented as punctate (~0.5–1.0 μm), solid structures that often co-localized with anti-tubulin immunofluorescence. These immunoreactive particles may be fragments of manchettes undergoing further processing within the spermatid cytoplasm.

The association of intense cytoplasmic dynein immunofluorescence in Sertoli cytoplasm with periods of peak secretory activity and the cytoplasmic dynein immunolocalization to ectoplasmic specializations suggest that cytoplasmic dynein plays an important and stage-dependent role in Sertoli cell function. The localization of cytoplasmic dynein and kinesin to manchettes strongly supports the argument that these microtubule-dependent mechanoenzymes are important for spermatid maturation.

ACKNOWLEDGMENTS

We kindly thank Michael Sheetz for providing a ready supply of anti-cytoplasmic dynein antibody, Scott Brady and George Bloom for supplying the anti-kinesin antibodies, and Ken Reuhl for supplying the HNK-1.

REFERENCES

1. Dym M, Fawcett DW. The blood-testis barrier in the rat and the physiological compartmentation of the seminiferous epithelium. Biol Reprod 1970; 3:308–326.
2. Dym M. The fine structure of the monkey *Macacao* Sertoli cell and its role in maintaining the blood-testis barrier. Anat Rec 1973; 175:639–656.
3. Setchell BP. The secretion of fluid by the testes of rats, rams and goats with some observations on the effect of age, cryptorchidism and hypophysectomy. J Reprod Fertil 1970; 23:79–85.
4. Hagenäs L, Ritzén EM, Plöen L, Hansson V, French FS, Nayfeh SN. Sertoli cell origin of testicular androgen-binding protein (ABP). Mol Cell Endocrinol 1975; 2:339–350.
5. Vernon RG, Kopec B, Fritz IB. Observations on the binding of androgens by rat testis seminiferous tubules and testis extracts. Mol Cell Endocrinol 1974; 1:167–187.
6. Skinner MK, Griswold MD. Sertoli cells synthesize and secrete transferrin-like protein. J Biol Chem 1980; 255:9523–9525.
7. Wright WW, Musto NA, Mather JP, Bardin CW. Sertoli cells secrete both testis-specific and serum proteins. Proc Natl Acad Sci 1981; 78:7565–7569.
8. Au CL, Robertson DM, De Kretser DM. An in-vivo method for estimating inhibin production by adult rat testes. J Reprod Fertil 1984; 71:259–265.
9. Au CL, Irby dC, Robertson DM, De Kretser DM. Effects of testosterone on testicular inhibin and fluid production in intact and hypophysectomized adult rats. J Reprod Fertil 1986; 76:257–266.
10. Leblond CP, Clermont Y. Definition of the stages of the cycle of the seminiferous epithelium in the rat. Ann NY Acad Sci 1952; 55:548–573.
11. Mather JP, Gunsalus GL, Musto NA, Cheng CY, Parvinen M, Wright W, Perez-Infante V, Margioris A, Liotta A, Becker R, Krieger DT, Bardin CW. The hormonal and cellular control of Sertoli cell secretion. J Steroid Biochem 1983; 19:41–51.
12. Rindler MJ, Ivanov I, Sabatini DD. Microtubule-acting drugs lead to the polarized delivery of the influenza hemagglutinin to the cell surface of polarized Madin Darby Canine kidney cells. J Cell Biol 1987; 104:231–241.
13. Achler C, Filmer D, Merte C, Drenkhahn D. Role of microtubules in polarized delivery of apical membrane proteins to the brush border of the intestinal epithelium. J Cell Biol 1989; 109:179–189.
14. Eilers U, Klumperman J, Hauri H-P. Nocodazole, a microtubule active drug, interferes with apical protein delivery in cultured intestinal epithelial cells (Caco-2). J Cell Biol 1989; 109:13–22.
15. Allen RD, Metuzals J, Tasaki I, Brady ST, Gilbert SP. Fast axonal transport in squid giant axon. Science 1982; 218:1127–1129.
16. Brady ST, Lasek RJ, Allen RD. Fast axonal transport in extruded axoplasm from the squid giant axon. Science 1982; 218:1129–1131.
17. Brady ST, Lasek RJ, Allen RD. Video microscopy of fast axonal transport in extruded axoplasm: A new model for study of molecular mechanisms. Cell Motil 1985; 5:81–101.
18. Hayden JH, Allen RD. Detection of single microtubules in living cells: particle transport can occur in both directions along the same microtubule. J Cell Biol 1984; 99:1785–1793.
19. Allen C, Borisy GG. Structural polarity and directional growth of microtubules of *Chlamydomonas* flagella. J Mol Biol 1974; 90:381–402.
20. Redenbach DM, Vogl AW. Microtubule polarity in Sertoli cells: a model for microtubule based spermatid transport. Eur J Cell Biol 1991; 54:277–290.
21. Burton PR, Paige JL. Polarity of axoplasmic microtubules in the olfactory nerve of the frog. Proc Natl Acad Sci 1981; 78:3269–3273.
22. Euteneuer U, McIntosh JR. Polarity of midbody and phragmoplast microtubules. J Cell Biol 1980; 87:509–515.

23. Paschal BM, Vallee RB. Retrograde transport by the microtubule-associated protein MAP 1C. Nature 1987; 330:181–183.
24. Vale RD, Schnapp BJ, Reese TS, Sheetz MP. Organelle, bead, and microtubule translocations promoted by soluble factors from the squid giant axon. Cell 1985; 40:559–569.
25. Vale RD, Reese TS, Sheetz MP. Identification of a novel force-generating protein, kinesin, involved in microtubule-based motility. Cell 1985; 42:39–50.
26. Saxton WM, Porter ME, Cohn SA, Scholey JM, Raff EC, McIntosh JR. *Drosophila* kinesin: characterization of microtubule motility and ATPase. Proc Natl Acad Sci 1988; 85:1109–1113.
27. Scholey JM, Porter ME, Grissom PM, McIntosh JR. Identification of kinesin in sea urchin eggs, and evidence for its localization in the mitotic spindle. Nature 1985; 318:483–486.
28. Murofushi H, Ikai A, Okuhara K, Kotani S, Aizawa H, Kumakura K, Sakai H. Purification and characterization of kinesin from bovine adrenal medulla. J Biol Chem 1988; 263:12744–12750.
29. Dabora SL, Sheetz MP. The microtubule-dependent formation of a tubulovesicular network with characteristics of the ER from cultured cell extracts. Cell 1988; 54:27–35.
30. Hering G, Borisy GG. Localization of kinesin to vesicles and reticular elements in cultured cells. J Cell Biol 1988; 107:673a.
31. Collins CA, Vallee RB. Preparation of microtubules from rat liver and testis: cytoplasmic dynein is a major microtubule associated protein. Cell Motil Cytoskel 1989; 14:491–500.
32. Vale RD, Schnapp BJ, Mitchison TJ, Steuer E, Reese TS, Sheetz MP. Different axoplasmic proteins generate movement in opposite directions along microtubules in vitro. Cell 1985; 43:623–632.
33. Vale RD, Schnapp BJ, Mitchison T, Steuer E, Reese TS, Sheetz MP. Different axoplasmic proteins generate movement in opposite directions along microtubules in vitro. Cell 1985; 43:623–632.
34. Vale RD, Scholey JM, Sheetz MP. Kinesin: Possible biological roles for a new microtubule motor. Trends Biochem Sci 1986; 11:464–468.
35. Steuer ER, Wordeman L, Schroer TA, Sheetz MP. Localization of cytoplasmic dynein to mitotic spindles and kinetochores. Nature 1990; 345:266–268.
36. Vale RD, Hotani H. Formation of membrane networks in vitro by kinesin-driven microtubule movement. J Cell Biol 1988; 107:2233–2241.
37. Pratt MM, Hisanaga S, Begg DA. An improved purification method for cytoplasmic dynein. J Cell Biochem 1984; 26:19–33.
38. Lye RJ, Porter ME, Scholey JM, McIntosh JR. Identification of a microtubule-based cytoplasmic motor in the nematode C. elegans. Cell 1987; 51:309–319.
39. Euteneuer U, Koonce MP, Pfister KK, Schliwa M. An ATPase with properties expected for the organelle motor of the giant amoeba, *Reticulomyxa*. Nature 1988; 332:176–178.
40. Koonce MP, McIntosh JR. Identification and immunolocalization of cytoplasmic dynein in *Dictyostelium*. Cell Motil Cytoskel 1990; 15:51–62.
41. Scroeder CC, Fok AK, Allen RD. Isolation of a cytoplasmic dynein from *Paramecium*. J Cell Biol 1989; 109:157a.
42. Schnapp BJ, Reese TJ. Dynein is the motor for retrograde axonal transport and organelles. Proc Natl Acad Sci 1989; 86:1548–1552.
43. Pfarr CM, McIntosh JR. HeLa cytoplasmic dynein is a microtubule translocator. J Cell Biol 1988; 107:244a.
44. Neely DM, Boekelheide K. Sertoli cell processes have axoplasmic features: an ordered microtubule distribution and an abundant high molecular weight microtubule-associated protein (cytoplasmic dynein). J Cell Biol 1988; 107:1767–1776.
45. Neely DM, Erickson HP, Boekelheide K. HMW-2, the Sertoli cell cytoplasmic dynein from rat testis, is a dimer composed of nearly identical subunits. J Biol Chem 1990; 265:8691–8698.
46. Paschal BM, Shpetner HS, Vallee RB. MAP 1C is a microtubule-activated ATPase which translocates microtubules in vitro and has dynein-like properties. J Cell Biol 1987; 105:1273–1282.
47. Schroer TA, Steuer ER, Sheetz MP. Cytoplasmic dynein is a minus-end-directed motor for membranous organelles. Cell 1989; 56:937–946.
48. Schnapp BJ, Reese TS. Dynein is the motor for retrograde axonal transport of organelles. Proc Natl Acad Sci 1989; 86:1548–1552.
49. Cande WZ, Wolniak SM. Chromosome movement in lysed mitotic cells in inhibited by vanadate. J Cell Biol 1978; 79:573–580.
50. Cande WZ, McDonald K. Physiological and ultrastructural analysis of elongating mitotic spindles reactivated in vitro. J Cell Biol 1986; 103:593–604.
51. Vogl AW. Distribution and function of organized concentrations of actin filaments in mammalian spermatogenic cells and Sertoli cells. Int Rev Cyt 1988; 119:1–56.
52. Russell L. Observations on rat Sertoli ectoplasmic ('junctional') specializations in their association with germ cells of the rat testis. Tissue Cell 1977; 9:475–498.
53. Christensen AK. Microtubules in Sertoli cells of the guinea pig testis. Anat Rec 1965; 151:335a.
54. Fawcett, D.W. Ultrastructure and function of the Sertoli cell. In: Hamilton DW, Greep RO (eds.), Handbook of Physiology and Endocrinology, section 7. Washington, DC: American Physiologic Society; 1975: 21–55.
55. Grove BD, Vogl AW. Sertoli cell ectoplasmic specializations: a type of actin-associated adhesion junction? J Cell Sci 1989; 93:309–323.
56. Vogl AW, Soucy LJ, Lew GJ. Distribution of actin in isolated seminiferous epithelia and denuded tubule walls of the rat. Anat Rec 1985; 213:63–71.
57. Brokelmann J. Fine structure of germ cells and Sertoli cells during the cycle of the seminiferous epithelium in the rat. Z Zellforsch Microsk Anat 1963; 59:820–850.
58. Vogl AW, Soucy LJ. Arrangement and possible function of actin filament bundles in ectoplasmic specializations of ground squirrel Sertoli cells. J Cell Biol 1985; 100:814–825.
59. Suarez-Quian CA, Dym M. Detection of microfilaments in rat Sertoli cell ectoplasmic specializations with NBD-phallicidin. Int J Androl 1988; 11:301–312.
60. Russell LD, Ettlin RA, Hikim APS, Clegg ED. Histological and Histopathological Evaluation of the Testis, Clearwater, FL:Cache River Press; 1990: 63–118.
61. Goodrowe KL, Heath E. Disposition of the manchette in the normal equine spermatid. Anat Rec 1984; 209:177–183.
62. Sickels KI, Heath E. Disposition of the manchette and related events in the feline spermatid. Anat Rec 1986; 216:367–372.
63. Dooher GB, Bennett D. Spermiogenesis and spermatozoa in sterile mice carrying different lethal T/t haplotypes: a transmission and scanning electron microscopy study. Biol Reprod 1977; 17:269–288.
64. Meistrich ML, Trostle-Weige PK, Russell LD. Abnormal manchette development in spermatids of azh/azh mutant mice. Am J Anat 1990; 188:74–86.
65. Russell LD, Russell JA, MacGregor GR, Meistrich ML. Linkage of manchette microtubules to the nuclear envelope and observations of the role of the manchette in nuclear shaping during spermiogenesis in rodents. Am J Anat 1991; 192:97–120.
66. Fawcett DW, Anderson WA, Phillips DM. Morphogenetic factors influencing the shape of the sperm head. Dev Biol 1971; 26:220–251.
67. Asa CS, Phillips DM. Nuclear shaping in spermatids of the Thai leaf frog *Megophrys montana*. Anat Rec 1988; 220:287–290.
68. Rattner JB, Brinkley BR. Ultrastructure of mammalian spermiogenesis. III. The organization and morphogenesis of the manchette during rodent spermiogenesis. J Ultrastruct Res 1972; 41:209–218.
69. Laemmli UK. Cleavage of structural proteins during the assembly of the head of bacteriophage T4. Nature 1970; 227:680–685.
70. Heukeshoven J, Dernick R. Improved silver staining procedure for fast staining in PhastSystem development unit. I. Staining of sodium dodecyl sulfate gels. Electrophoresis 1988; 9:23–33.
71. Hollenbeck PJ. The distribution, abundance and subcellular localization of kinesin. J Cell Biol 1989; 108:2335–2342.
72. Pfister KK, Wagner MC, Stenoien DL, Brady ST, Bloom GS. Monoclonal antibodies to kinesin heavy and light chains stain vesicle-like structures, but not microtubules, in cultured cells. J Cell Biol 1989; 108:1453–1463.
73. Kuznetsov SA, Gelfand VI. Bovine brain kinesin is a microtubule-activated ATPase. Proc Nat Acad Sci USA 1986; 83:8530–8534.
74. Amos LA. Kinesin from pig brain studied by electron microscopy. J Cell Sci 1987; 87:105–111.
75. Virtanen I, Ekblom P, Laurila P. Subcellular compartmentalization of saccharide moieties in cultured normal and malignant cells. J Cell Biol 1980; 85:429–434.
76. Lipsky NG, Pagano RE. A vital stain for the Golgi apparatus. Science 1985; 228:745–747.
77. Amlani S, Vogl AW. Changes in the distribution of microtubules and intermediate filaments in mammalian Sertoli cells during spermatogenesis. Anat Rec 1988; 220:143–160.